

Structure and solvatochromism of heteroaromatic aminoketones containing thiophene moieties

Mohamed El-Sayed,¹ Bernhard Walfort,² Heinrich Lang,² Wolfgang Poppitz³ and Stefan Spange^{1*}

¹Department of Polymer Chemistry, Institute of Chemistry, Chemnitz University of Technology, Strasse der Nationen 62, D-09111 Chemnitz, Germany

²Department of Inorganic Chemistry, Institute of Chemistry, Chemnitz University of Technology, Strasse der Nationen 62, D-09111 Chemnitz, Germany.

³Institute of Inorganic and Analytical Chemistry, Jena Friedrich-Schiller University, August-Bebel Strasse 2, 07743 Jena, Germany

Received 19 April 2005; revised 21 June 2005; accepted 23 June 2005

ABSTRACT: A series of *N*-substituted phenyl-2-thienyl ketones including 2-(4-fluorobenzoyl)thiophene (FLBT, **1a**), 2-(4-piperidinobenzoyl)thiophene (PIBT, **1b**), 2-(4-morpholinobenzoyl)thiophene (MOBT, **1c**), 2-(4-thiomorpholinobenzoyl)thiophene (THBT, **1d**), 2-(4-phenylpiperazinobenzoyl)thiophene (PHBT, **1e**), 2-(4-pyrrolidinobenzoyl)thiophene (PYBT, **1f**), 2-(4-hydroxyethylpiperazinobenzoyl)thiophene (HYBT, **1g**), 1,4-bis(4-benzoyl-2-thienyl)piperazine (BBTP, **2**) and 1,6-bis(4-benzoyl-2-thienyl)-*N,N'*-dimethylhexamethylenediamine (BBDA, **3**) have been investigated regarding solvatochromism and solid-state structure. Solvatochromic properties have been analyzed using the Kamlet–Taft linear solvation energy relationship. The influence of the dipolarity/polarizability (π^*) and hydrogen-bond acidity (α) of the solvent, respectively, on the portions of the bathochromic UV–Vis band shift as a function of substituent is discussed. The solid-state structures of **1b** (C₁₆H₁₇NOS), **1c** (C₁₅H₁₅NO₂S) and **1f** (C₁₅H₁₅NOS) have been determined by single-crystal x-ray structure analysis. Crystallochromic effects are discussed comparatively with regard to the linear solvation energy relationships and the results of the solid-state structures. Copyright © 2005 John Wiley & Sons, Ltd.

KEYWORDS: LSE correlations; heteroaromatic ketones; solvatochromism; substituent effects; solid-state structures; thiophenes; x-ray crystal structure analysis

INTRODUCTION

The search for organic compounds that are suitable for defined nano-aggregation with quantum effects remains empirical and still requires a lot of conceptual work, as shown by recent activities.^{1–4} It seems that the use of non-symmetrically arranged organic substituents, which are associated with a significant change in the physical properties, is required to achieve structural transition from a single molecule to a nanocrystal.

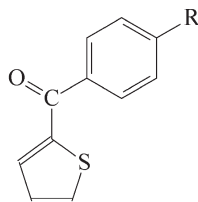
For this purpose, organic chromophores have been investigated because optical properties related to size effects can be measured readily and reproducibly. In order to achieve a quantum leap in the construction of this type of condensed phase, highly polarizable organic molecules are needed that show significant changes in colour as a function of environmental influences. It is

therefore of importance to establish correlations between structural parameters of organic solids and optical properties as a function of structure variations.^{5–15} Some of the results in this area are obtained by our group using dipolar aromatic aminoketones of furan and thiophene derivatives that are functionalized in the periphery of the molecule.⁵

Similar compounds have a wide range of application in the field of non-linear optical materials and nanotechnology devices.^{6–8} Because the ground-state aromaticity of the thiophene is lower than that of 4-*N,N*-dimethylaminophenyl, and the solubility of thiophenes is usually higher than that of the parent benzene compounds, much attention has been paid recently to chromophoric and solvatochromic compounds that contain thiophene moieties.^{5–9}

Michler's ketone derivatives appeared to be particularly attractive because they can be synthesized readily from 4,4'-difluorobenzophenone and secondary amines under mild reaction conditions.^{15–17} Furthermore, these types of compounds have been investigated widely because of their solvatochromic and photophysical properties^{15–25} as well as their use as precursors for producing di- and triphenylmethylium ions.^{26–28}

*Correspondence to: S. Spange, Department of Polymer Chemistry, Institute of Chemistry, Chemnitz University of Technology, Strasse der Nationen 62, D-09111 Chemnitz, Germany.
E-mail: stefan.spange@chemie.tu-chemnitz.de
Contract/grant sponsors: DFG; Fonds der Chemischen Industrie; Chemnitz University of Technology.



No.	Name	Abb.	Substituent
1a	2-(4-fluorobenzoyl)thiophene	FLBT	F
1b	2-(4-piperidinobenzoyl)thiophene	PIBT	
1c	2-(4-morpholinobenzoyl)thiophene	MOBT	
1d	2-(4-thiomorpholinobenzoyl)thiophene	THBT	
1e	2-(4-phenylpiperazinobenzoyl)thiophene	PHBT	
1f	2-(4-pyrrolidinobenzoyl)thiophene	PYBT	
1g	2-(4-hydroxyethylpiperazinobenzoyl)thiophene	HYBT	
1h	[4-di(2-acetoxyethyl)aminophenyl]-2-thienylmethanone	Thi(OAc) ₂	
1i	[4-di(2-hydroxyethyl)aminophenyl]-2-thienylmethanone	Thi(OH) ₂	

Scheme 1. The heteroaromatic ketones **1(a–g)** used in this work. Compounds **1h** and **1i** were taken from Ref. 5 for comparison

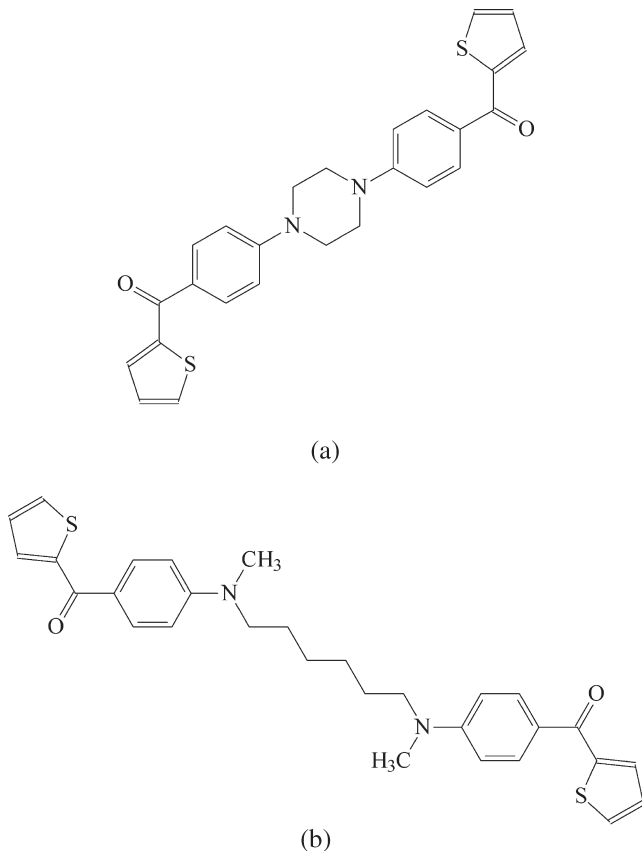
In this paper we report on the synthesis of compounds **1(d–g)**, **2** and **3** and their spectroscopic characteristics, which are compared with those of **1a**, **1h** {[4-di(2-acetoxyethyl)aminophenyl]-2-thienylmethanone, Thi(OAc)₂}⁵ and **1i** {[4-di(2-hydroxyethyl)aminophenyl]-2-thienylmethanone, Thi(OH)₂}⁵, from previous work (Schemes 1 and 2). The linking of two identical solvatochromic chromophors by a rigid (piperazine) or a flexible (*N,N'*-dimethylhexamethylenediamine) spacer was also used as a model to study both the influence of molecular dipolarity and the flexibility of the chromophoric moieties on each other (Scheme 2).

To quantify the environmental effects on the optical properties of these compounds, the well-established and accepted Kamlet–Taft linear solvation energy

(LSE) relationship has been used.^{29–39} The simplified Kamlet–Taft equation applied to single solvatochromic shifts, $XYZ = 1/\lambda_{\max} = \tilde{\nu}_{\max}(\text{probe})$,^{32,36–39} is given in Eqn (1):

$$XYZ = (XYZ)_0 + a\alpha + b\beta + s(\pi^* + d\delta) \quad (1)$$

where $(XYZ)_0$ is the solute property of a reference system, e.g. a non-polar medium, α describes the hydrogen-bond donating (HBD) ability, β describes the hydrogen-bond accepting (HBA) ability, π^* is the dipolarity/polarizability of the respective solvent, δ is a polarizability correction term (which is 1.0 for aromatic, 0.5 for polyhalogenated and zero for aliphatic solvents) and a , b , s and d are solvent-independent regression



Scheme 2. Structural formulae of (a) 1,4-bis(4-benzoyl-2-thienyl)piperazine (BBTP, **2**) and (b) 1,6-bis(4-benzoyl-2-thienyl)-*N,N'*-dimethylhexamethylenediamine (BBDA, **3**)

coefficients.^{32,37,38} The objective of this work is to investigate the influence of the substituents on the dipolarity and basicity of the target compounds and how these effects can be measured by the LSE relationship.

RESULTS AND DISCUSSION

Solvatochromic measurements

The UV–Vis absorption spectra of the solvatochromic UV–Vis band (the longest-wavelength band of the π – π^* transition) of compounds **1(a–g)**, **2** and **3** have been measured in 37 various solvents at 293 K and the spectroscopic results are summarized in Table 1.

A representative UV–Vis spectral series for compound **1f** in five different solvents is shown in Fig. 1(a) and a collection of UV–Vis spectra for every compound studied, measured in 1,4-dioxane, is shown in Fig. 1(b).

The UV–Vis absorption band for PIBT, MOBT, THBT, PHBT, PYBT, HYBT **1(b–g)**, BBTP (**2**) and BBDA (**3**) undergoes a significant bathochromic shift of the long-wavelength UV–Vis band with increasing solvent polarity from cyclohexane to water (Table 1). According to Michler's ketone, the 2-thienyl aminophenyl ketones also show a positive solvatochromism that is significantly

a function of the dipolarity/polarizability and HBD ability of the solvent. Compared with other compounds, for **1a** and **1g** the extent of the positive solvatochromic shift is smaller.

Because unprecedented UV–Vis absorption band shifts as a function of solvent polarity are obtained for **1a** and **1g**, the solvatochromism of these compounds will be discussed separately (*vide infra*).

Results of the multiple square analyses of the measured $\tilde{\nu}_{\max}$ values of the 2-thienyl aminophenyl ketones with the Kamlet–Taft solvent parameters are summarized in Table 2 (the empirical Kamlet–Taft solvent parameters were taken from the literature⁴⁰ according to previous work). The $\tilde{\nu}_{\max}$ values measured in formic acid for all compounds were excluded from the solvatochromic LSE correlations because chemical alteration (protonation at the amino nitrogen atom) takes place.

The calculated LSE relationship is of high quality, as indicated particularly by correlation coefficients of 0.90 for special mathematical functions of $\tilde{\nu}_{\max}$ with α , β and π^* , respectively.

Multiple square analyses for compounds **1(b–f)**, **2** and **3** show that the influence of the β term can be ignored because of the smaller value of coefficient b and the high error in this value. However, the effect of β on $\tilde{\nu}_{\max}$ for **1a** and **1g** is more pronounced and significantly evident.

It should be emphasized at this point that the solvatochromic properties of compounds **2** and **3** fit well into this concept, showing the importance of the individual chromophoric system for the respective solvatochromic property. The long-wavelength UV–Vis absorption maximum of compound **2** (Table 2) ranges from $\lambda_{\max} = 328$ nm in triethylamine to $\lambda_{\max} = 396$ nm in 1,1,1,3,3,3-hexafluoroisopropanol (HFIP), corresponding to $\Delta\lambda = +68$ nm ($\Delta\tilde{\nu}_{\max} = -5240$ cm⁻¹), whereas in the case of compound **3** the shift ranges from $\lambda_{\max} = 345$ nm in triethylamine to $\lambda_{\max} = 407$ nm in HFIP, corresponding to $\Delta\lambda = +62$ nm ($\Delta\tilde{\nu}_{\max} = -4500$ cm⁻¹). Thus, these compounds show the same solvatochromic effect as found for monosubstituted 2-thienyl aminophenyl ketones, which means that the solvatochromism of the bichromophoric compound can be treated like that containing a single chromophore.

The specific solvation of the HBD solvent at the HBA substituent 2-hydroxyethyl piperazine compensates for the influence of HBD attack at the carbonyl oxygen on the extent of the bathochromic shift.

The best regression fit obtained for compound **1g** in 30 solvents is given by Eqn (2) after removing the $\tilde{\nu}_{\max}$ values of HBD solvents 1-butanol, acetic acid, formamide, ethane-1,2-diol, benzyl alcohol and water from the regression analysis.

$$\begin{aligned} \tilde{\nu}_{\max} \times 10^{-3} [\text{HYBT}] \\ = 30.321 - 0.552 \alpha - 0.553 \beta - 2.112 \pi^* \quad (2) \\ r = 0.967 \quad n = 30 \quad \text{SD} = 0.170 \quad F < 0.0001 \end{aligned}$$

Table 1. UV–Vis absorption maxima of compounds **1(a–g)**, **2** and **3** measured in 37 solvents^a of different polarity and hydrogen bond ability

Solvent	$\tilde{\nu}_{\max}$ 1a (10 ³ cm ^{−1})	$\tilde{\nu}_{\max}$ 1b (10 ³ cm ^{−1})	$\tilde{\nu}_{\max}$ 1c (10 ³ cm ^{−1})	$\tilde{\nu}_{\max}$ 1d (10 ³ cm ^{−1})	$\tilde{\nu}_{\max}$ 1e (10 ³ cm ^{−1})	$\tilde{\nu}_{\max}$ 1f (10 ³ cm ^{−1})	$\tilde{\nu}_{\max}$ 1g (10 ³ cm ^{−1})	$\tilde{\nu}_{\max}$ 2 (10 ³ cm ^{−1})	$\tilde{\nu}_{\max}$ 3 (10 ³ cm ^{−1})
Formic acid	30.86	30.03	30.03	30.49	28.33	31.15	28.09	29.15	30.77
Triethylamine	33.22	29.24	30.21	29.67	30.03	28.65	29.67	30.49	29.07
Cyclohexane	33.44	29.15	30.40	29.76	30.12	28.82	30.12	30.03	28.90
Diethyl ether	31.65	29.07	30.03	29.33	29.41	28.41	29.50	29.41	28.49
Tetrachloromethane	33.67	28.82	29.94	29.15	29.59	28.09	29.67	29.50	28.33
Ethyl acetate	34.01	28.57	29.67	28.90	29.41	27.93	29.24	28.90	28.09
<i>p</i> -Xylene	33.00	28.49	29.50	28.82	29.24	27.86	29.24	28.99	28.17
Toluene	33.56	28.41	29.24	28.65	29.15	27.78	29.15	28.90	28.09
1,4-Dioxane	33.78	28.41	29.50	28.57	29.24	27.86	29.07	28.82	28.01
1,2-Dimethoxyethane	33.44	28.41	29.41	28.57	29.15	27.78	29.07	28.65	27.93
Tetrahydrofuran	33.00	28.33	29.41	28.57	29.15	27.78	28.99	28.57	27.93
Benzene	33.56	28.25	29.33	28.49	28.99	27.62	29.07	28.65	27.93
Acetone	30.03	27.93	28.90	28.33	28.57	27.40	28.65	28.17	27.55
Acetonitrile	33.11	27.78	28.99	28.25	28.82	27.32	28.57	28.01	27.32
Anisole	30.86	27.78	28.65	27.93	27.93	27.40	28.57	28.01	27.47
1,2-Dichloroethane	33.67	27.62	28.99	28.17	28.65	27.03	28.57	28.09	27.25
Dichloromethane	33.56	27.55	28.99	28.17	28.65	26.95	28.57	28.17	27.25
<i>N,N</i> -Dimethylacetamide	33.44	27.55	28.65	27.86	28.41	27.03	28.25	27.70	27.03
1-Decanol	31.15	27.47	28.90	28.01	28.49	26.88	28.49	27.78	27.03
Chloroform	33.67	27.47	29.07	28.17	28.65	26.88	28.82	28.17	27.17
Ethanol	31.35	27.47	28.49	27.62	28.17	26.67	28.09	27.47	26.81
Tetramethyl urea	30.96	27.47	28.57	27.78	28.01	26.88	27.86	27.62	27.03
<i>N,N</i> -Dimethylformamide	33.44	27.47	28.65	27.86	28.33	26.88	28.17	27.70	27.03
Pyridine	32.05	27.40	28.41	27.78	28.25	26.81	28.09	27.78	26.95
4-Butyrolactone ^b	31.15	27.32	28.33	27.78	28.17	26.74	27.86	27.40	26.88
Benzonitrile	30.86	27.32	28.41	27.70	28.17	26.67	28.09	27.55	26.88
1-Butanol	31.35	27.25	28.49	27.47	28.01	26.60	27.93	27.25	26.74
1,1,2,2-Tetrachloroethane	33.56	27.03	28.65	27.78	28.25	26.60	28.25	27.70	26.81
Methanol	33.67	27.03	28.57	27.47	28.09	26.53	28.09	27.32	26.67
Dimethylsulfoxide	33.44	27.03	28.25	27.40	27.93	26.60	27.78	27.17	26.67
Acetic acid	33.78	26.88	28.49	27.40	28.82	26.25	29.85	27.25	26.46
Formamide	32.89	26.46	27.78	26.81	27.40	25.91	29.15	26.60	26.04
Ethane-1,2-diol	33.67	26.39	27.70	26.81	27.40	25.97	29.15	26.67	26.11
Benzyl alcohol	30.21	26.32	27.62	26.74	27.17	25.77	27.47	26.53	26.04
2,2,2-Trifluoroethanol	31.25	25.91	27.78	26.74	27.55	25.38	27.70	26.39	25.58
1,1,1,3,3,3-Hexafluoro-2-propanol	31.06	24.57	26.95	26.04	26.74	24.21	28.17	25.25	24.57
Water	33.33	^c	28.65	^c	^c	^c	29.24	^c	^c

^a The α , β and π^* values for all solvents were taken from Ref. 47.^b Solvatochromic parameters for this solvent were taken from Ref. 39.^c The probe is insoluble in this solvent.

It is worth noting that the $\tilde{\nu}_{\max}$ values of compound **1a** in 17 selected solvents (see footnotes of Table 2) correlate significantly with the single β parameter, as indicated by the following equation:

$$\tilde{\nu}_{\max} \times 10^{-3} [\text{FLBT}] = 33.766 - 2.164 \beta \quad (3)$$

$$r = 0.818 \quad n = 17 \quad \text{SD} = 0.454 \quad F < 0.0001$$

On increasing the Hammett σ^+ -substituent constant,²⁶ an increase of a is expected.^{41p} This would indicate an increase in the basicity of the carbonyl oxygen atom. The value of coefficient a decreases in the order: BBTP > PIBT > PYBT > BBDA > THBT > Thi(OAc)₂

> PHBT > MOBT > Thi(OH)₂ > FLBT > HYBT (see Table 2 and Ref. 5), which is roughly in line with the electron donor strength of the substituents.²⁶

This result, in accordance with our previous studies,^{15,16} shows that nitrogen-linked CH₂CH₂OH groups in the periphery of the chromophore cause an increase of the positive mesomeric effect when interacting with HBA solvents. The significant influence of the β term (HBA solvent property) compared with the HBD term of the solvent on the bathochromic shift of the UV–Vis band indicates qualitatively a different solvation. In strong HBD solvents, such as water, acetic acid and HFIP, a strong hypsochromic shift of the UV–Vis band is observed, which shows that the positive mesomeric effect of

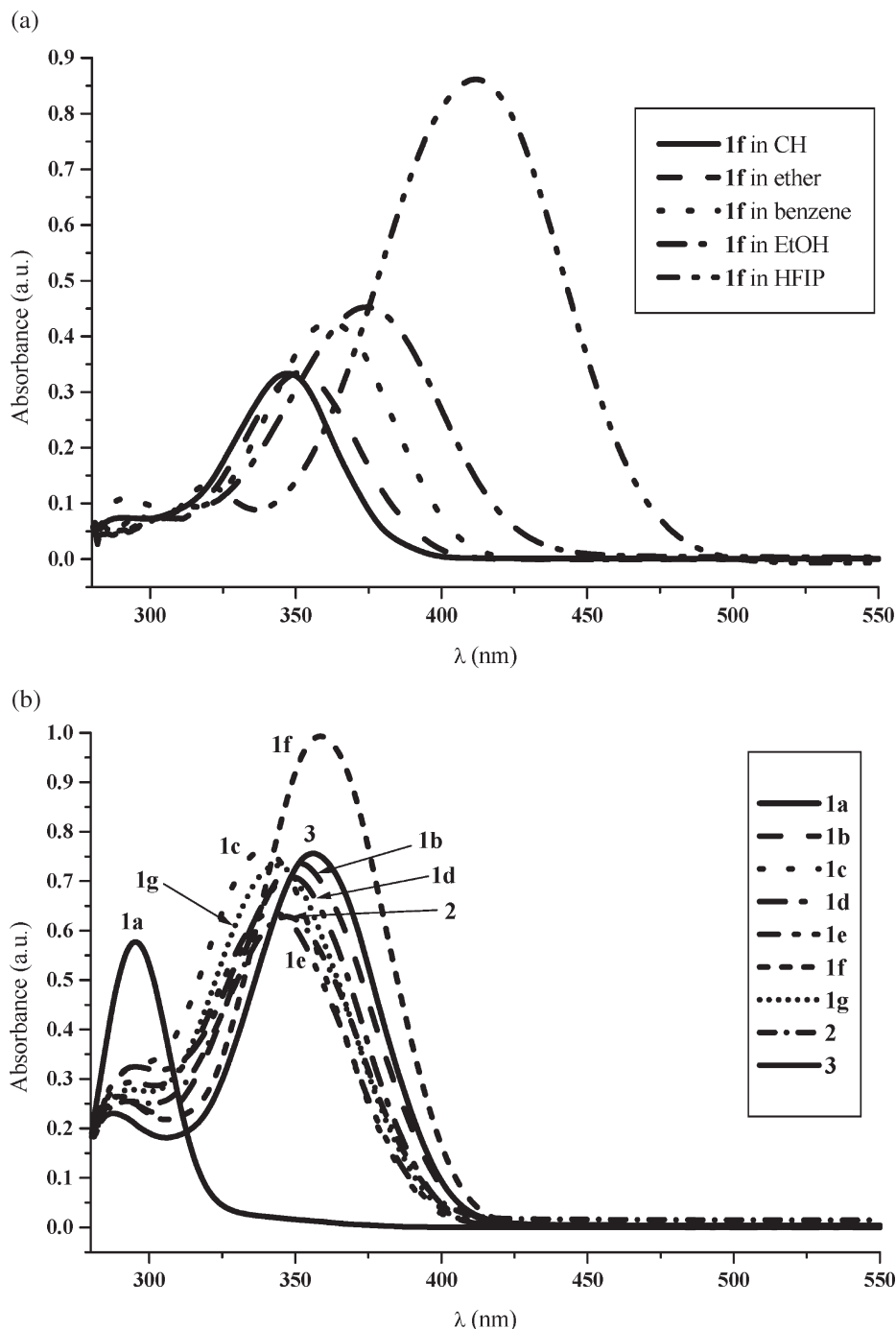


Figure 1. The UV-Vis absorption spectra of 10^{-5} mol l^{-1} solutions of (a) compounds **1f** in different solvents, i.e. cyclohexane (CH), diethylether, benzene, ethyl alcohol (EtOH), and 1,1,1,3,3,3-hexafluoro-2-propanol (HFIP), and (b) compounds **1(a-g)**, **2** and **3** in 1,4-dioxane

the nitrogen atom at the aromate in compound **1g** is suppressed. Generally, the results are in accord with the LSE results for Michler's ketone.

X-ray crystal structure analysis of compounds **1b**, **1c** and **1f**

X-ray structure analyses have been determined for compounds **1b**, **1c** and **1f**. The crystallographic data are listed

in Table 3 and the solid-state structures of compounds **1b**, **1c** and **1f** are shown in Figs 2–4. Compound **1b** crystallizes from ethyl acetate at 50°C as yellow plates (see Experimental section) in the monoclinic space group $P2_1$, with $a = 640.63(9)$, $b = 770.85(10)$ and $c = 1427.56(19)$ pm, $\beta = 99.235(3)^\circ$, $V = 695.83(16) \times 10^6 \text{ pm}^3$ and $Z = 2$ (Fig. 2).

Molecule **1c** crystallizes from a saturated ethyl acetate solution at 50°C as light-yellow rods in the triclinic space group $P-1$, with $a = 1004.74(8)$, $b = 1067.73(9)$

Table 2. Values of the solvent-independent correlation coefficients a , b and s of the Kamlet–Taft parameters α , β and π^* , respectively. The solute property of a reference system $(XYZ)_0$, standard deviation (SD), significance (F) and number of solvents (n) for the solvatochromism of compounds **1(a–g)**, **2** and **3**

Compound	$(XYZ)_0$	a	b	s	r	SD	Probe $> F$	n
1a	33.372	−0.523	−0.973	−0.283	0.323	1.219	0.3108	36 ^a
	33.293	—	−0.941	−0.446	0.238	1.232	0.3818	36 ^a
	33.707	−1.019	−1.514	0.041	0.882	0.340	0.0002	17 ^b
	33.766	—	−2.164	—	0.818	0.454	<0.0001	17 ^b
	33.642	—	−0.896	−0.703	0.334	1.076	0.3451	21 ^c
1b	29.465	−1.390	0.287	−2.384	0.973	0.233	<0.0001	35 ^d
	29.553	−1.395	—	−2.335	0.970	0.243	<0.0001	35 ^d
	29.546	—	0.170	−2.485	0.974	0.168	<0.0001	21 ^c
	29.579	—	—	−2.429	0.972	0.169	<0.0001	21 ^c
	30.419	−0.811	−0.114	−1.916	0.912	0.324	<0.0001	36 ^a
1c	30.384	−0.809	—	−1.935	0.911	0.320	<0.0001	36 ^a
	30.585	—	−0.090	−2.226	0.967	0.178	<0.0001	21 ^a
	30.568	—	—	−2.255	0.966	0.175	<0.0001	21 ^c
	29.905	−1.117	−0.141	−2.264	0.981	0.169	<0.0001	35 ^d
	29.862	−1.114	—	−2.288	0.980	0.171	<0.0001	35 ^d
1d	29.903	—	−0.023	−2.371	0.983	0.132	<0.0001	21 ^c
	29.899	—	—	−2.379	0.983	0.128	<0.0001	21 ^c
	30.295	−0.875	−0.183	−2.182	0.929	0.302	<0.0001	35 ^d
	30.240	−0.872	—	−2.214	0.927	0.301	<0.0001	35 ^d
	30.278	—	−0.082	−2.244	0.941	0.243	<0.0001	21 ^c
1e	30.262	—	—	−2.271	0.941	0.238	<0.0001	21 ^c
	28.870	−1.361	0.198	−2.291	0.976	0.214	<0.0001	35 ^d
	28.930	−1.365	—	−2.258	0.974	0.218	<0.0001	35 ^d
	28.961	—	0.136	−2.434	0.981	0.141	<0.0001	21 ^c
	28.987	—	—	−2.390	0.980	0.142	<0.0001	21 ^c
1f	29.916	−0.139	−0.548	−1.451	0.640	0.539	0.0007	36 ^a
	29.895	—	−0.539	−1.494	0.631	0.536	0.0002	36 ^a
	30.324	—	−0.443	−2.187	0.974	0.163	<0.0001	21 ^c
	30.239	—	—	−2.332	0.960	0.196	<0.0001	21 ^c
	30.343	−1.411	−0.165	−2.860	0.975	0.250	<0.0001	35 ^d
2	30.293	−1.408	—	−2.888	0.974	0.251	<0.0001	35 ^d
	30.412	—	−0.002	−3.111	0.974	0.214	<0.0001	21 ^c
	30.412	—	—	−3.112	0.974	0.209	<0.0001	21 ^c
	29.139	−1.331	0.057	−2.351	0.979	0.200	<0.0001	35 ^d
	29.156	−1.332	—	−2.341	0.979	0.198	<0.0001	35 ^d
3	29.227	—	0.039	−2.514	0.979	0.157	<0.0001	21 ^c
	29.234	—	—	−2.502	0.978	0.153	<0.0001	21 ^c

^aThe $\tilde{\nu}_{\max}$ values for formic acid are excluded.^bThe $\tilde{\nu}_{\max}$ values for triethylamine, cyclohexane, tetrachloromethane, *p*-xylene, toluene, 1,2-dimethoxyethane, tetrahydrofuran, benzene, acetonitrile, 1,2-dichloroethane, dichloromethane, chloroform, pyridine, 1-butanol, 1,1,2,2-tetrachloroethane and formamide are used for the correlation.^cSolvents with $\alpha = 0$ are used in the correlation.^dSee footnotes c in Table 1 and a in Table 2.

and $c = 1318.61(11)$ pm, $\alpha = 76.086(2)$, $\beta = 85.300(2)$, $\gamma = 85.476(2)^\circ$, $V = 1365.90(2) \times 10^6 \text{ pm}^3$ and $Z = 4$ (Fig. 3).

Compound **1f** crystallizes from a chloroform–ethyl acetate (1:2) mixture at 25°C as yellow blocks in the monoclinic space group $P2_1$, with $a = 628.75(8)$, $b = 747.12(10)$ and $c = 1393.91(18)$ pm, $\beta = 99.031(3)^\circ$, $V = 646.67(15) \times 10^6 \text{ pm}^3$ and $Z = 2$ (Fig. 4).

The N1–C9 interatomic distance in compound **1f** is smaller [$135.6(3)$ pm] than the N1–C9 length in compound **1b** [$138.8(3)$ pm], indicating a stronger conjugation of the lone pair of electrons at the nitrogen atom with the benzene ring in compound **1f**. However, the N1–C9 separation in compound **1c** is the longest one [$139.2(2)$

pm] and this is due to the more electronegative oxygen atom of the morpholino group. This result is in accordance with the UV–Vis spectroscopic results of these compounds in solution. A bathochromic shift is observed in the order of **1f** > **1b** > **1c** using the same solvent. The strong participation of the carbonyl group in two hydrogen bonds results in an elongation of the C=O distance in compound **1i** [$d_{\text{C=O}} = 124.76(14)$ pm]⁵ in comparison with compounds **1b** [$d_{\text{C=O}} = 124.00(3)$ pm] **1c** [$d_{\text{C=O}} = 122.90(19)$ pm] and **1f** [$d_{\text{C=O}} = 122.8(2)$ pm], where no hydrogen bond to the oxygen atom of the carbonyl group occurs. In compound **1f**, the C4–C5–C6 angle [$\gamma = 120.24(16)^\circ$] is less than that in compound **1b** [$\gamma = 121.4(2)^\circ$] or compound **1c** [$\gamma = 121.03(14)^\circ$].

Table 3. Crystal data, details of the data collection and structure analysis of compounds **1b**, **1c** and **1f**

	1b	1c	1f
Crystal color, shape	Yellow, plate	Light yellow, rod	Yellow, block
Crystal size (mm)	0.4 × 0.3 × 0.05	0.7 × 0.4 × 0.3	0.7 × 0.4 × 0.05
Empirical formula	C ₁₆ H ₁₇ NOS	C ₁₅ H ₁₅ NO ₂ S	C ₁₅ H ₁₅ NOS
Chemical formula	C ₁₆ H ₁₇ NOS	C ₁₅ H ₁₅ NO ₂ S	C ₁₅ H ₁₅ NOS
Formula weight	271.37	273.34	257.34
Crystal system	Monoclinic	Triclinic	Monoclinic
Space group	<i>P</i> 2 ₁	<i>P</i> -1	<i>P</i> 2 ₁
Unit cell dimensions (pm), with angles (°) in parentheses	<i>a</i> = 640.63(9) <i>b</i> = 770.85(10) <i>c</i> = 1427.56(19) α = 90 β = 99.235(3) γ = 90	<i>a</i> = 1004.74(8) <i>b</i> = 1067.73(9) <i>c</i> = 1318.61(11) α = 76.086(2) β = 85.300(2) γ = 85.476(2)	<i>a</i> = 628.75(8) <i>b</i> = 747.12(10) <i>c</i> = 1393.91(18) α = 90 β = 99.031(3) γ = 90
Volume (10 ⁶ pm ³)	695.83(16)	1365.90(2)	646.67(15)
<i>Z</i>	2	4	2
Density (calculated) (g cm ⁻³)	1.295	1.329	1.322
Absorption coefficient (mm ⁻¹)	0.224	0.234	0.237
<i>F</i> (000)	288	576	272
Goodness-of-fit on <i>F</i> ²	0.949	1.022	1.016
Collected reflections	5378	9603	5713
Independent reflections	2747	5321	2560
θ range for data collection (°)	1.45–26.02	1.59–25.93	2.96–26.09
Completeness to maximum θ (%)	99.9	99.7	99.9
Index ranges	$-7 \leq h \leq 7, -9 \leq k \leq 9, 0 \leq l \leq 17$	$-12 \leq h \leq 12, -12 \leq k \leq 13, 0 \leq l \leq 17$	$-7 \leq h \leq 7, -9 \leq k \leq 9, 0 \leq l \leq 17$
Final <i>R</i> indices <i>R</i> ₁ / <i>wR</i> ₂ [<i>I</i> ≥ 2σ(<i>I</i>)]	0.0418/0.0860	0.0401/0.0991	0.0334/0.0726
<i>R</i> indices <i>R</i> ₁ / <i>wR</i> ₂ (all data)	0.0714/0.0951	0.0613/0.1110	0.0484/0.0785
Max./min. electron density (10 ⁻⁶ electron × pm ⁻³)	0.141/−0.163	0.166/−0.205	0.101/−0.160

These differences are due to a conformation change induced by the N-substituent effect at the 4-position of the phenyl ring.

The torsion angles for compound **1b** resemble −24.8(4)° (C8—C9—N1—C12) and 155.9(3)° (C10—C9—N1—C12), whereas in compound **1f** the values are 7.4(3)° (C10—C9—N1—C15) and −171.9(2)° (C8—C9—N1—C15). These data demonstrate that the terminal piperidino group in compound **1b** is tilted more than the terminal pyrrolidino group in compound **1f** with respect to the 2-benzoyl thiophene moiety. This result also explains the larger electron-donating density of **1f** compared with **1b**.

In the solid-state, the piperidino phenyl, morpholino phenyl and pyrrolidino phenyl groups in compounds **1b**, **1c** and **1f** are twisted in a different way around the planar ketone substituent C4—C5—O1—C6, indicated by torsional angles for O1—C5—C6—C7 and O1—C5—C6—C11 of 14.2(4)° and −162.6(3)° in compound **1b**, 26.7(2)° and −152.26(17)° in compound **1c** and 163.5(2)° and −13.1(3)° in compound **1f**. Hence, the piperidino, morpholino and pyrrolidino phenyl entities are bent with respect to the carbonyl plane. Thus, the conformational differences of compounds **1b**, **1c** and **1f** in the solid-state seem responsible for the differences in the UV–Vis reflectance spectra of these molecules (*vide infra*).

Also, the thienyl group is twisted in compounds **1b**, **1c** and **1f** around the planar ketone substituent, with different values for the torsional angles of S1—C4—C5—O1 and C3—C4—C5—O1: 29.9(3) and −145.9(3) in compound **1b**, 13.0(2) and −162.6(6) in compound **1c** and −34.1(3) and 142.5(2) in compound **1f**. The sulfur atom and the carbonyl oxygen in all x-ray structures are oriented toward the same side, in agreement with the conformational studies on, for example, 2-benzoyl thiophene.⁴²

The C5—C6 interatomic distances in compounds **1b** [147.1(3) pm] and **1f** [146.5(3) pm] and the C1—C6 distances in compound **1i** [145.5(15) pm] are smaller than the C4—C5 interatomic distances of 148.2(4) and 147.9(3) pm for **1b** and **1f** and the C1—C2 distance in **1i** [147.5(15) pm]. However, in compound **1c** the C5—C6 distance [148.4(2) pm] is longer than the C4—C5 distance [146.9(2) pm]. This indicates that the extent of π -conjugation with the carbonyl is higher for the phenylene group than the thienyl group in compounds **1b**, **1f** and **1i**. Conformational studies on 2-benzoylthiophene have shown that the extent of π -conjugation with the carbonyl is higher for the heteroaromatic ring,⁴² which explains the influence of the N-substituent on the resonance structure of the heteroaromatic aminoketones.

The crystal packing diagrams for compounds **1b**, **1c** and **1f** are shown in Figs 3(b), 4(b) and 5(b). A significant

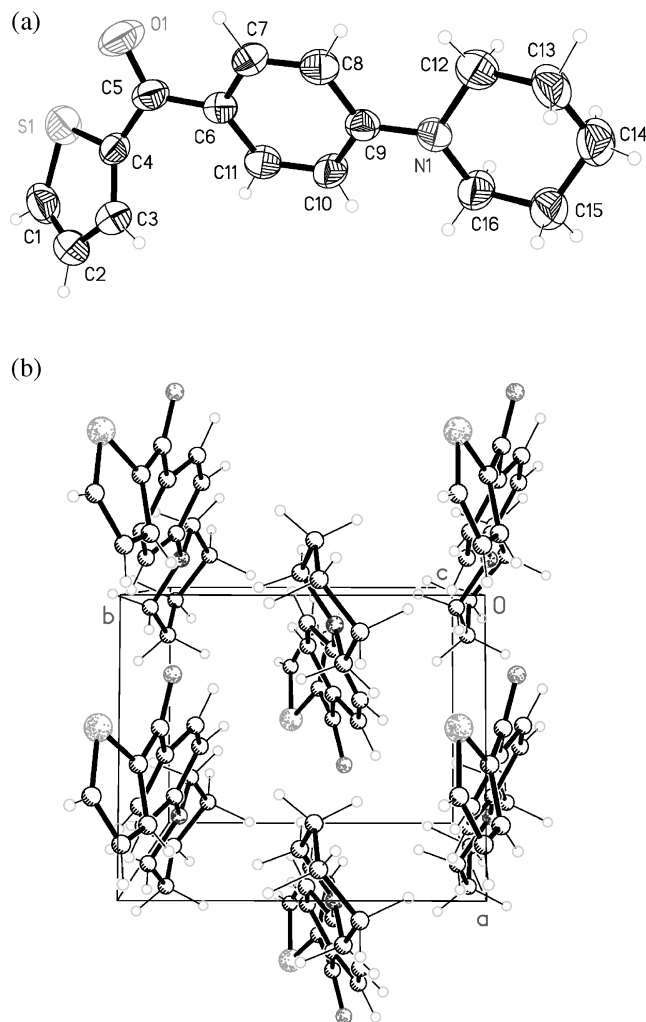


Figure 2. Crystal structure of 2-(4-piperidinobenzoyl)thiophene **1b**

change was observed in the unit cell lengths and unit cell volumes due to the substituent effect. Moreover, the crystal system is changed in compound **1c** (triclinic) in comparison with compounds **1b** and **1f**, which are both monoclinic. The unit cell of compound **1c** contains two geometrically similar but crystallographically independent molecules and the interatomic bond distances and angles are identical within standard derivations for both molecules.

The UV–Vis diffuse reflectance spectra of crystal powders of compounds **1(a–g)**, **2** and **3**

The UV–Vis reflectance spectra of compounds **1(a–g)**, **2** and **3** are depicted in Fig. 5. The UV–Vis absorption bands are, however, broad and exhibit fine structures. This phenomenon could be due to coupling of the fundamental π – π^* electronic transition with vibrational levels of the excited-state^{43a} or Davydov splitting of the exciton levels.^{43b–e}

Although compounds **1(a–g)** show only a single UV–Vis band in the longest-wavelength region ($\lambda_{\text{max}} = 336, 354, 358, 347, 349, 351$ and 351 nm for **1a**, **1b**, **1c**, **1d**, **1e**, **1f**, and **1g**, respectively), compounds **2** and **3** show two UV–Vis bands at 366 and 443 nm for **2** and at 338 and 394 nm for **3**. The λ_{max} value in the solid-state is even blue-shifted by 13 – 62 nm (see Table 1 and Fig. 5) compared with the absorption spectra of the **1(b–f)** solutions in the strongest polar solvent HFIP. This result can be explained by Kasha's molecular exciton theory.⁴³ The interaction of parallel out-of-phase transition dipoles leads to an energy level lower than that of the isolated molecules, whereas the interaction of parallel in-phase transition dipoles leads to a higher energy level. Transition from the ground state to the lower exciton state (out-of-phase) is forbidden, whereas transition from the ground state to the higher exciton state (in-phase) is allowed. These parallel transition dipoles therefore cause the blue-shifted absorption bands.

As can be seen from Fig. 5, compound **2** exhibits a red-shifted UV–Vis absorption band maximum in comparison with compound **3**. This result is attributed to the through-space interaction between the two chromophores in the solid-state structure of compound **2**.¹⁵ However, this type of interaction is not found in compound **3** and the presence of the second band in compound **3** is likely to be attributed to the presence of strong intermolecular π – π stacking interactions in the solid-state between the aromatic moieties that is responsible for minimizing the electrostatic energy.^{43c} The charge-transfer transitions may contribute to this new UV–Vis absorption band.

CONCLUSION

The synthesis of novel carbonyl-spaced solvatochromic chromophores has been carried out and their solvatochromic properties in solution and the solid-state structure of compounds **1b**, **1c** and **1f** have been determined. The solvent influence on the position of the solvatochromic UV–Vis absorption band depends on the nature (polarity, basicity and sterical requirements) of the (+M)-substituent. The stronger the (+M)-effect of the substituent, the larger is the extent of the solvatochromic effect induced by the HBD capacity of the solvent. In non-HBD solvents, the value of coefficient s decreases in the order of $2 > 3 > 1b > 1f > 1d > 1g > 1e > 1c > 1i > 1h > 1a$ (see Table 2 and Ref. 5).

These results indicate that the presence of two heteroaromatic aminoketone solvatochromic moieties in one system enhances the influence of the dipolarity/polarizability. Also, as shown from Table 2, the s value is governed by the nature of the spacer, with $s = -3.112$ and -2.502 for compounds **2** (rigid spacer) and **3** (flexible spacer), respectively.

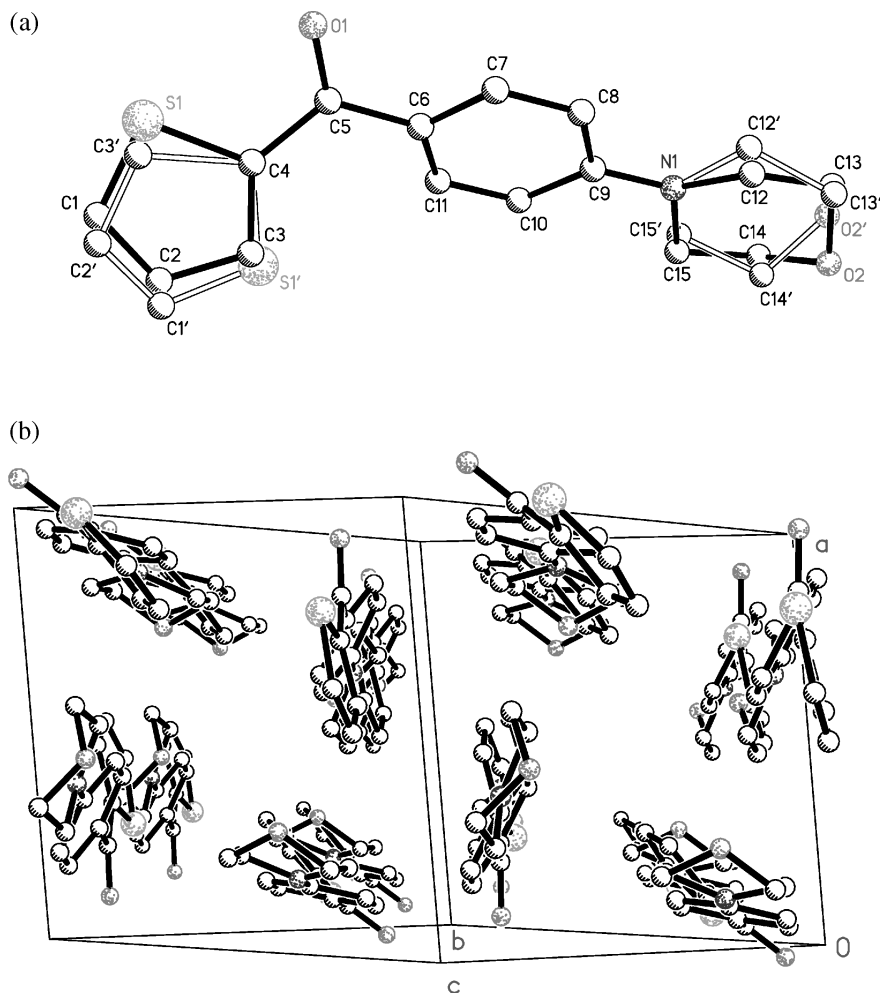


Figure 3. Crystal structure of 2-(4-morpholinobenzoyl)thiophene **1c**

EXPERIMENTAL

Materials

Solvents from Merck, Fluka, Lancaster and Aldrich were redistilled over appropriate drying agents prior to use.^{37,44} The 2-(4-fluorobenzoyl)thiophene **1a** from Acros (purity 97%) was crystallized from ethyl acetate–*n*-hexane (1:1) before use.

Spectral measurements

The UV–Vis absorption spectra were recorded by means of a UV–Vis MCS 400 diode-array spectrometer from Carl Zeiss Jena connected to an immersion cell (TSM 5) via glass-fiber optics. A diffuse reflectance accessory was attached to the spectrometer for diffuse reflectance measurements, which were carried out with properly characterized powdered samples, using BaSO₄ powder as a reference.⁵ The UV–Vis spectra give an average of all

orientations of the crystal powder because diffuse light was used.

The NMR measurements were recorded at 20 °C on a Varian GEMINI 300 FT NMR spectrometer operating at 300 MHz for ¹H and at 75 MHz for ¹³C. The signals of the solvent (CDCl₃) were used as internal standards. Electro-spray ionization mass spectra were obtained with a Finnigan MATSSQ 710 spectrometer.

Correlation analysis

Multiple regression analysis was performed with the Origin 5.0 statistic programs.

Crystal Structure Determinations

Crystal data for the structures of compounds **1b**, **1c** and **1f** are presented in Table 3. Data for all structures were collected on a Bruker-axs Smart 1K diffractometer at

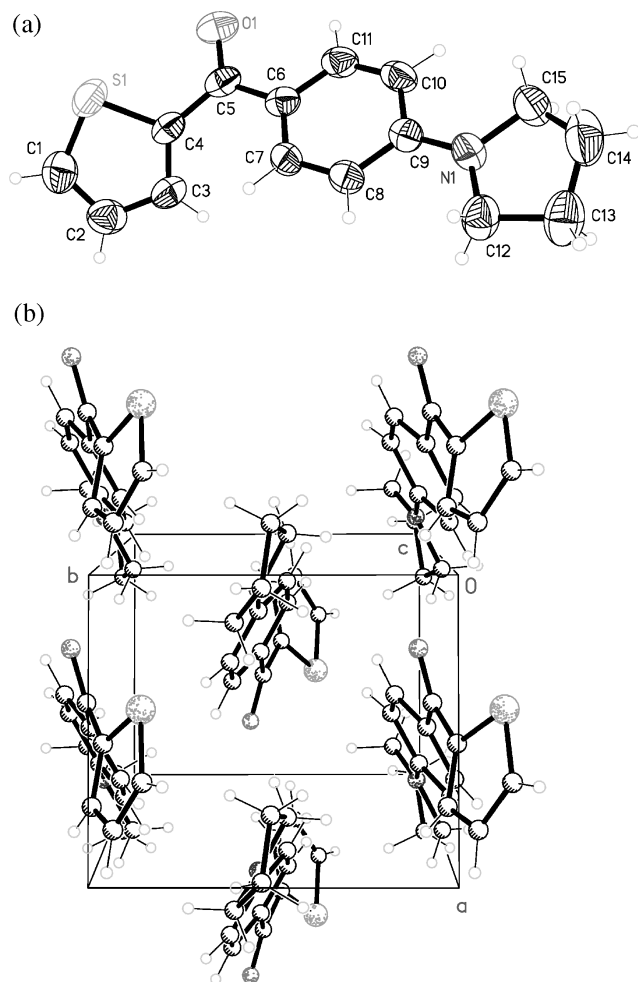


Figure 4. Crystal structure of 2-(4-pyrrolidinobenzoyl)thiophene **1f**

room temperature using Mo K α radiation ($\lambda = 0.71073$ Å). The structures were determined by direct methods using SHELXS 97⁴⁵ and refined by full-matrix least-squares procedures on F² using SHELXL 97.⁴⁶ All non-hydrogen atoms were refined anisotropically. A riding model was employed in the refinement of the hydrogen atom positions of compound **1c**. Hydrogen atom positions in compounds **1b** and **1f** have been taken from the difference Fourier map and refined freely. Refinement of the Flack x parameters⁴⁷ in compound **1b** to $-0.01(8)$ and in compound **1f** to $0.03(8)$, respectively, confirm the right absolute structure for both. In compound **1c** the thiophene and the morpholine groups are disordered and have been refined to split occupancies of 0.79/0.21 (S1—C3), 0.68/0.32 (C12—C15), 0.76/0.24 (S2—C18) and 0.30/0.61/0.09 (C27—C30), respectively. The disordered groups have been aligned with similarity restraints. Other crystallographic data (excluding structure factors) for the structures reported in this paper have been deposited with the Cambridge Crystallographic Data Center as a supplementary publication (CCDC numbers: **1b**, 255591; **1c**, 255589; **1f**, 255590). Copies of the data can be obtained free of charge on application

to the CCDC, 12 Union Road, Cambridge CB2 1EZ, UK (Fax: +44(1223)336-033; E-mail: deposit@ccdc.cam.ac.uk).

General procedure for preparation of compounds **1(b–g)**

A solution of 2-(4-fluorobenzoyl)thiophene **1a** (6.22 g, 35 mmol) in anhydrous dimethylsulfoxide (50 ml) was added at 25 °C to a mixture of the appropriate secondary amine (piperidine, morpholine, thiomorpholine, phenylpiperazine, pyrrolidine, *N*-hydroxyethylpiperazine) (35 mmol) and potassium carbonate (9.81 g, 71 mmol) in the same solvent (70 ml). The mixture was refluxed for 24 h at 140 °C. After cooling to room temperature, the mixture was poured into ice water and neutralized with 2 N HCl (20 ml). The precipitate was filtered off, washed with water and crystallized from ethyl acetate–*n*-hexane (1:1) to give the pure title compounds **1(b–g)**.

2-(4-Piperidinobenzoyl)thiophene 1b. Yield (8.35 g, 87.9%), m.p. 127 °C, yellow crystals. C₁₆H₁₇NOS (271.37) (calc. C, 70.82%; H, 6.3%; N, 5.2%; S, 11.8%; found: C, 70.6%; H, 6.3%; N, 5.1%; S, 12.0%); MS (ESI), $m/z = 272.1$ [$M^+ + 1$]; ¹H-NMR (CDCl₃): δ 7.84 (d, $J = 8.79$ Hz, 2H, ArH-2,6), 7.62 (d, $J = 4.4$ Hz, 2H, ThH-3',4'), 7.12 (dd, $J = 3.85, 4.94$ Hz, 1H, ThH-5'), 6.86 (d, $J = 8.79$ Hz, 2H, ArH-3,5), 3.36 (t, $J = 5.49$ Hz, 4H, NCH₂), 1.64 (s, broad, 6H, NCH₂CH₂CH₂); ¹³C-NMR (CDCl₃): δ 186.16 (C=O), 154.15 (ArC-4), 144.18 (ThC-2'), 133.12 (ArC-2,6), 132.42 (ThC-3'), 131.66 (ThC-5'), 127.47 (ArC-1), 126.48 (ThC-4'), 113.24 (ArC-3,5), 48.53 (NCH₂), 25.27 (NCH₂CH₂), 24.25 (NCH₂CH₂CH₂).

2-(4-Morpholinobenzoyl)thiophene 1c. Yield (8.85 g, 92.5%), m.p. 114 °C, pale yellow crystals. C₁₅H₁₅NO₂S (273.34) (calc. C, 65.9%; H, 5.5%; N, 5.1%; S, 11.7%; found: C, 66.0%; H, 5.5%; N, 5.1%; S, 12.0%); MS (ESI), $m/z = 274.1$ [$M^+ + 1$]; ¹H-NMR (CDCl₃): δ 7.86 (d, $J = 8.79$ Hz, 2H, ArH-2,6), 7.62 (d, $J = 4.4$ Hz, 2H, ThH-3',4'), 7.12 (dd, $J = 3.85, 4.94$ Hz, 1H, ThH-5'), 6.89 (d, $J = 8.79$ Hz, 2H, ArH-3,5), 3.84 (t, $J = 4.94$ Hz, 4H, OCH₂), 3.29 (t, $J = 4.94$ Hz, 4 H, NCH₂); ¹³C-NMR (CDCl₃): δ 186.35 (C=O), 153.90 (ArC-4), 143.93 (ThC-2'), 133.45 (ArC-2,6), 132.86 (ThC-3'), 131.45 (ThC-5'), 128.14 (ArC-1), 127.58 (ThC-4'), 113.28 (ArC-3,5), 66.47 (OCH₂), 47.46 (NCH₂).

2-(4-Thiomorpholinobenzoyl)thiophene 1d. Yield (8.75 g, 86.4%), m.p. 85 °C, dark yellow crystals. C₁₅H₁₅NOS₂ (289.41) (calc. C, 62.3%; H, 5.2%; N, 4.8%; S, 22.2%; found: C, 62.2%; H, 5.0%; N, 4.7%; S, 22.0%); MS (ESI), $m/z = 290.1$ [$M^+ + 1$]; ¹H-NMR (CDCl₃): δ 7.88 (d, $J = 9.00$ Hz, 2H, ArH-2,6), 7.66 (d, $J = 4.4$ Hz, 2H, ThH-3',4'), 7.15 (dd, $J = 3.85, 4.94$ Hz, 1H, ThH-5'), 6.87 (d,

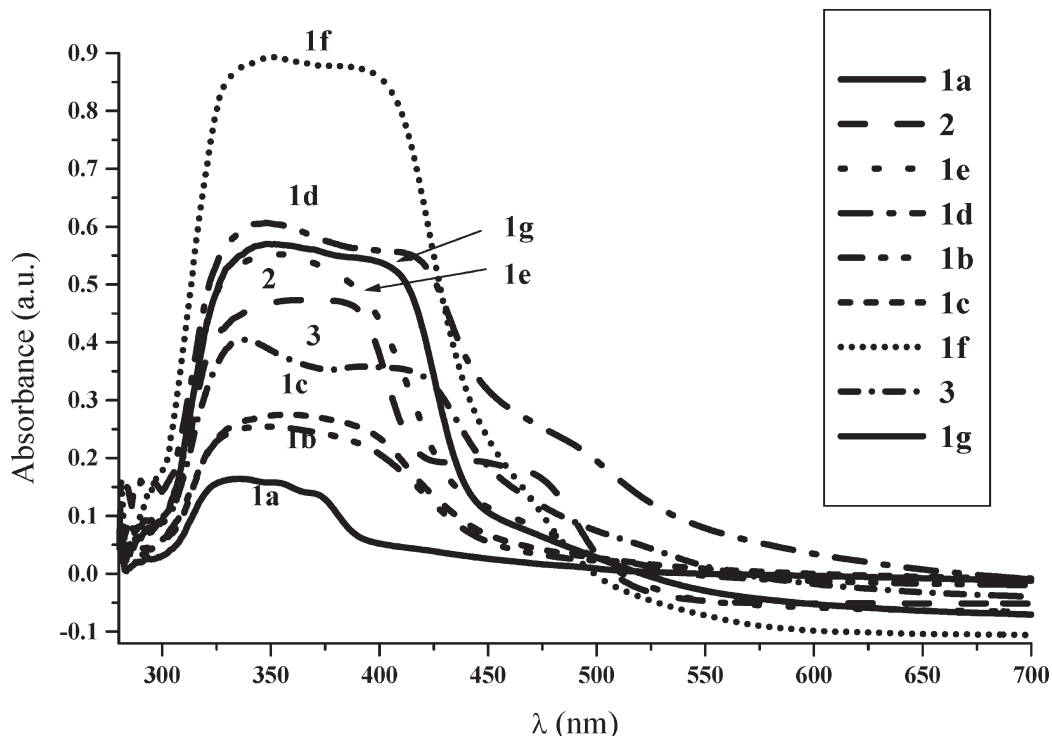


Figure 5. The UV-Vis absorption spectra of compounds **1(a-g)**, **2** and **3** as crystals

$J = 9.00$ Hz, 2H, ArH-3,5), 3.80 (t, $J = 5.21$ Hz, 4H, SCH₂), 2.72 (t, $J = 5.21$, 4H, NCH₂); ¹³C-NMR (CDCl₃): δ 186.56 (C=O), 153.21 (ArC-4), 144.52 (ThC-2'), 133.75 (ArC-2,6), 133.17 (ThC-3'), 132.26 (ThC-5'), 128.05 (ArC-1), 127.72 (ThC-4'), 114.20 (ArC-3,5), 50.80 (SCH₂), 26.27 (NCH₂).

2-(4-Phenylpiperazinobenzoyl)thiophene 1e. Yield (11.15 g, 91.4%), m.p. 138 °C, pale yellow crystals. C₂₁H₂₀N₂OS (348.46) (calc. C, 72.4%; H, 5.8%; N, 8.0%; S, 9.2%; found: C, 72.2%; H, 5.7%; N, 8.1%; S, 9.4%); MS (ESI), $m/z = 349.1$ [M⁺ + 1]; ¹H-NMR (CDCl₃): δ 7.95 (d, $J = 9.00$ Hz, 2H, ArH-2,6), 7.69 (d, $J = 4.58$ Hz, 2H, ThH-3',4'), 7.35 (dd, $J = 7.27$, 8.85 Hz, 2H, ArH-9,11), 7.19 (dd, $J = 3.85$, 4.94 Hz, 1H, ThH-5'), 7.01 (dd, $J = 6.00$, 15.00 Hz, 5H, ArH-3,5,8,10,12), 3.57 (t, $J = 5.53$ Hz, 4H, H—C₁, H—C₄ piperazine protons), 3.39 (t, $J = 5.53$ Hz, 4H, H—C₂, H—C₃ piperazine protons); ¹³C-NMR (CDCl₃): δ 186.78 (C=O), 154.19 (ArC-4), 151.20 (ArC-7), 144.56 (ThC-2'), 133.86 (ArC-2,6), 133.25 (ThC-3'), 132.04 (ArC-1), 129.07 (ThC-5'), 128.50 (ArC-9,11), 128.06 (ThC-4'), 120.92 (ArC-10), 116.85 (ArC-8,12), 114.14 (ArC-3,5), 49.60 (C₁, C₄ piperazine carbons), 47.89 (C₂, C₃ piperazine carbons).

2-(4-Pyrrolidinobenzoyl)thiophene 1f. Yield (8.50 g, 94.4%), m.p. 174 °C, pale yellow crystals. C₁₅H₁₅NOS (257.35) (calc. C, 70.01%; H, 5.9%; N, 5.4%; S, 12.46%; found: C, 70.0%; H, 5.7%; N, 5.4%; S, 12.6%); MS (ESI), $m/z = 258.1$ [M⁺ + 1]; ¹H-NMR (CDCl₃): δ 7.87 (d,

$J = 8.79$ Hz, 2H, ArH-2,6), 7.60 (d, $J = 4.4$ Hz, 2H, ThH-3',4'), 7.11 (dd, $J = 3.85$, 4.94 Hz, 1H, ThH-5'), 6.53 (d, $J = 8.79$ Hz, 2H, ArH-3,5), 3.35 (t, $J = 6.59$ Hz, 4H, NCH₂), 2.02 (t, $J = 6.59$ Hz, 4H, NCH₂CH₂); ¹³C-NMR (CDCl₃): δ 186.04 (C=O), 150.76 (ArC-4), 144.42 (ThC-2'), 132.71 (ArC-2,6), 131.98 (ThC-3'), 131.93 (ArC-1), 127.35 (ThC-5'), 124.47 (ThC-4'), 110.64 (ArC-3,5), 47.47 (NCH₂), 25.35 (NCH₂CH₂).

2-(4-Hydroxyethylpiperazinobenzoyl)thiophene 1g. Yield (9.50 g, 85.8%), m.p. 106 °C, pale yellow crystals. C₁₇H₂₀N₂O₂S (316.41) (calc. C, 64.5%; H, 6.37%; N, 8.9%; S, 10.1%; found: C, 64.62%; H, 6.2%; N, 8.8%; S, 10.3%); MS (ESI), $m/z = 371.1$ [M⁺ + 1]; ¹H-NMR (CDCl₃): δ 7.84 (d, $J = 8.79$ Hz, 2H, ArH-2,6), 7.62 (d, $J = 4.4$ Hz, 2H, ThH-3',4'), 7.12 (dd, $J = 3.85$, 4.94 Hz, 1H, ThH-5'), 6.88 (d, $J = 8.79$ Hz, 2H, ArH-3,5), 3.66 (t, $J = 5.49$ Hz, 2H, OCH₂), 3.35 (t, $J = 4.94$ Hz, 4H, H—C₁, H—C₄ piperazine protons), 2.64 (t, $J = 5.49$ Hz, 2H, NCH₂CH₂O), 2.58 (t, $J = 4.94$ Hz, 4H, H—C₂, H—C₃ piperazine protons); ¹³C-NMR (CDCl₃): δ 186.32 (C=O), 153.73 (ArC-4), 143.93 (ThC-2'), 133.39 (ArC-2,6), 132.76 (ThC-3'), 131.48 (ArC-1), 127.63 (ThC-5'), 127.55 (ThC-4'), 113.43 (ArC-3,5), 59.37 (OCH₂), 57.78 (NCH₂CH₂O), 52.49 (C₂, C₃ piperazine carbons), 47.26 (C₁, C₄ piperazine carbons).

General procedure for preparation of compounds 2 and 3. A solution of anhydrous piperazine (1.51 g, 17.5 mmol) or *N,N*-dimethyl-1,6-hexanediamine (2.52 g,

17.5 mmol) in anhydrous dimethylsulfoxide (50 ml) was added at 25 °C to a mixture of 2-(4-fluorobenzoyl)thiophene **1a** (6.22 g, 35 mmol) and potassium carbonate (9.81 g, 71 mmol) in the same solvent (70 ml) and heated at 140 °C for 48 h. After cooling to room temperature, the crude reaction mixture is taken up in 0.09 N HCl solution (400 ml) and the precipitate formed was filtered off, washed three times with water, dried and crystallized from ethyl acetate–*n*-hexane (1:1) to afford analytically pure **2** and **3**.

1,4-Bis(4-benzoyl-2-thienyl)piperazine 2. Yield (6.00 g, 74.8%), m.p. 202 °C, light yellow crystals. C₂₆H₂₂N₂O₂S₂ (458.59) (calc. C, 68.10%; H, 4.84%; N, 6.11%; S, 14.0%; found: C, 67.65%; H, 4.78%; N, 6.10%; S, 14.09%); MS (ESI), *m/z* = 459.2 [M⁺ + 1]; ¹H-NMR (CDCl₃): δ 7.92 (d, *J* = 8.85 Hz, 4H, ArH-2,6,2',6'), 7.66 (d, *J* = 5.53 Hz, 4H, ThH-3,4,3',4'), 7.16 (t, 2H, ThH-5,5'), 6.96 (d, *J* = 8.85 Hz, 4H, ArH-3,5,3',5'), 3.58 (s, 8H, NCH₂); ¹³C-NMR (CDCl₃): δ 186.80 (C=O), 153.78 (ArC-4,4'), 144.49 (ThC-2,2'), 133.89 (ArC-2,6,2',6'), 133.34 (ThC-3,3'), 132.07 (ArC-1,1'), 128.73 (ThC-5,5'), 128.06 (ThC-4,4'), 114.00 (ArC-3,5,3',5'), 47.51 (NCH₂).

1,6-Bis(4-benzoyl-2-thienyl)-N,N'-dimethylhexamethylenediamine 3. Yield (7.00 g, 77.4%), m.p. 130 °C, light yellow crystals. C₃₀H₃₂N₂O₂S₂ (516.71) (calc. C, 69.7%; H, 6.24%; N, 5.42%; S, 12.41%; found: C, 69.26%; H, 6.16%; N, 5.38%; S, 12.51%); MS (ESI), *m/z* = 517.1 [M⁺ + 1]; ¹H-NMR (CDCl₃): δ 7.87 (d, *J* = 8.79 Hz, 4H, ArH-2,6,2',6'), 7.62 (dd, *J* = 4.94, 6.04 Hz, 4H, ThH-3,4,3',4'), 7.12 (t, 2H, ThH-5,5'), 6.65 (d, *J* = 8.79 Hz, 4H, ArH-3,5,3',5'), 3.39 (t, *J* = 7.69 Hz, 4H, NCH₂); 3.02 (s, 6H, NCH₃); 1.62 (m, 4H, NCH₂CH₂); 1.38 (m, 4H, NCH₂CH₂CH₂); ¹³C-NMR (CDCl₃): δ 185.92 (C=O), 152.15 (ArC-4,4'), 144.34 (ThC-2,2'), 132.80 (ArC-2,6,2',6'), 132.09 (ThC-3,3'), 131.93 (ArC-1,1'), 127.40 (ThC-5,5'), 124.77 (ThC-4,4'), 110.38 (ArC-3,5,3',5'), 52.21 (NCH₂), 38.42 (NCH₃), 26.92 (NCH₂CH₂), 26.84 (NCH₂CH₂CH₂).

Acknowledgements

Financial support by the DFG (Accumol research training group), the Fonds der Chemischen Industrie (Frankfurt am Main) and the Chemnitz University of Technology is gratefully acknowledged.

REFERENCES

1. Fu H-B, Yao J-N. *J. Am. Chem. Soc.* 2001; **123**: 1434–1439.
2. Xu C, Xue Q, Zhong Y, Cui Y, Ba L, Zhao B, Gu N. *Nanotechnology* 2002; **13**: 47–50.
3. Lu HM, Jiang Q. *J. Phys. Chem. B* 2004; **108**: 5617–5619.
4. Tian Z, Chen Y, Yang W, Yao J, Zhu L, Shuai Z. *Angew. Chem.* 2004; **116**: 4152–4155.
5. El-Sayed M, Müller H, Rheinwald G, Lang H, Spange S. *Chem. Mater.* 2003; **15**: 745–754.
6. (a) Rao VP, Jen AK-Y, Cai Y. *Chem. Commun.* 1996: 1237–1238; (b) Jen AK-Y, Rao VP, Drost K, Cai Y, Mininni RM, Kenney JT, Binkley ES, Dalton LR, Marder SR. *Proc. SPIE* 1994; **2143**: 321–340; (c) Würthner F, Wortmann R, Meerholz K. *Chem. Phys. Chem.* 2002; **3**: 17–31.
7. (a) Gilmour S, Montgomery RA, Marder SR, Cheng L-T, Jen AK-Y, Cai Y, Perry JW, Dalton LR. *Chem. Mater.* 1994; **6**: 1603–1604; (b) Jen AK-Y, Cai Y, Bedworth PV, Marder SR. *Adv. Mater.* 1997; **9**: 132–135; (c) Perry JW, Bourhill G, Marder SR, Lu D, Chen G, Goddard WA. *Polym Prepr. (Am. Chem. Soc., Div. Polym. Chem.)* 1994; **35**: 148–149.
8. Blenk M, Boldt P, Bräuchle C, Grahn W, Ledoux I, Nerenz H, Stadler S, Wichern J, Zyss J. *J. Chem. Soc., Perkin Trans. 2* 1996; 1377–1384.
9. (a) Bäuerle P, Würthner F, Heid S. *Angew. Chem. Int. Ed.* 1990; **29**: 419–420; (b) Effenberger F, Würthner F. *Angew. Chem. Int. Ed.* 1993; **32**: 719–721.
10. Horn D, Rieger J. *Angew. Chem. Int. Ed.* 2001; **40**: 4330–4361.
11. Tykwinski RR, Kamada K, Bykowski D, Hegmann FA, Hinkle RJ. *J. Opt. A: Pure Appl. Opt.* 2002; **4**: 202–206.
12. (a) Mataga N, Kubota T. *Molecular Interactions and Electronic Spectra*, Marcel Dekker: New York, 1970; (b) Lehn J-M. *Supramolecular Chemistry*, VCH: Weinheim, 1995.
13. Lacroix PG, Daran J-C, Cassoux P. *New J. Chem.* 1998; **22**: 1085–1091.
14. El-Sayed M, Müller H, Rheinwald G, Lang H, Spange S. *Monatsh. Chem.* 2003; **134**: 361–370.
15. El-Sayed M, Müller H, Rheinwald G, Lang H, Spange S. *J. Phys. Org. Chem.* 2001; **14**: 247–255.
16. Spange S, El-Sayed M, Müller H, Rheinwald G, Lang H, Poppitz W. *Eur. J. Org. Chem.* 2002; 4159–4168.
17. Beach SF, Hepworth JD, Jones P, Mason D, Sawyer J. *J. Chem. Soc., Perkin Trans. 2* 1989; 1087–1090.
18. Suppan P. *J. Chem. Soc., Faraday Trans. 1* 1975; **71**: 539–547.
19. Brown RG, Porter G. *J. Chem. Soc., Faraday Trans. 1* 1977; **73**: 1569–1573.
20. Groenen EJJ, Koelman WN. *J. Chem. Soc., Faraday Trans. 2* 1979; **7**: 58–68.
21. Spange S, Keutel D. *Liebigs Ann. Chem.* 1992; 423–428.
22. Spange S, Vilsmeier E, Adolph S, Fährmann A. *J. Phys. Org. Chem.* 1999; **12**: 547–556.
23. Spange S, Keutel D. *Liebigs Ann. Chem.* 1993; 981–985.
24. Barnabas MV, Liu A, Trifunac AD, Krongauz VV, Chang CT. *J. Phys. Chem.* 1992; **96**: 212–217.
25. (a) Zimmermann Y, El-Sayed M, Prause S., Spange S. *Monatsh. Chem.* 2001; **132**: 1347–1361; (b) El-Sayed M, Seifert A, Spange S. *J. Sol-Gel. Technol.* 2005; **34**: 77–94.
26. Mayr H, Bug T, Gotta MF, Hering N, Irrgang B, Janker B, Kempf B, Loos R, Ofial A, Remennikov G, Schimmel H. *J. Am. Chem. Soc.* 2001; **123**: 9500–9512.
27. Duxbury DF. *Chem. Rev.* 1993; **93**: 281–433.
28. Gorman SA, Hepworth JD, Mason D. *J. Chem. Soc., Perkin Trans. 2* 2000; 1889–1895.
29. Kamlet MJ, Taft RW. *J. Am. Chem. Soc.* 1976; **98**: 377–383.
30. Taft RW, Kamlet MJ. *J. Am. Chem. Soc.* 1976; **98**: 2886–2894.
31. Kamlet MJ, Abboud JL, Taft RW. *J. Am. Chem. Soc.* 1977; **99**: 6027–6038.
32. Kamlet MJ, Abboud JL, Abraham MH, Taft RW. *J. Org. Chem.* 1983; **48**: 2877–2887.
33. Kamlet MJ, Abraham MH, Doherty RM, Taft RW. *J. Am. Chem. Soc.* 1984; **106**: 464–466.
34. Kamlet MJ, Doherty RM, Abraham MH, Marcus Y, Taft RW. *J. Phys. Chem.* 1988; **92**: 5244–5255.
35. Kamlet MJ, Doherty RM, Carr PW, Mackay D, Abraham MH, Taft RW. *Environ. Sci. Technol.* 1988; **22**: 503–509.
36. Kamlet MJ. *J. Prog. Phys. Org. Chem.* 1993; **19**: 295–317.
37. Reichardt C. *Solvents and Solvent Effects in Organic Chemistry* (2nd edn). VCH: Weinheim, 1988.
38. Reichardt C. *Chem. Rev.* 1994; **94**: 2319–2358.
39. Abraham MH, Chadha HS, Whiting GS, Mitchell RC. *J. Pharm. Sci.* 1994; **83**: 1085–1100.
40. Marcus Y. *Chem. Soc. Rev.* 1993; **22**: 409–416.
41. Novaki LP, El Seoud OA. *Ber. Bunsen-Ges. Phys. Chem.* 1996; **100**: 648–655.

42. (a) Kaper L, Veenland JU, de Boer ThJ. *Spectrochim. Acta* 1967; **23A**: 2605–2608; (b) Cheng CL, John IJ, Ritchie GLD, Gore PH, Farnell L. *J. Chem. Soc., Perkin Trans. 2* 1975; **7**: 744–751; (c) Abu-Eittah R, Hilal R. *Bull. Chem. Soc. Jpn.* 1978; **51**: 2718–2723.
43. (a) Hotta S, Rughooputh SDDV, Heeger AJ, Wudl F. *Macromolecules* 1987; **20**: 212–215; (b) Koren AB, Curtis MD, Kampf JW. *Chem. Mater.* 2000; **12**: 1519–1522; (c) Würthner F, Yao S, Debaerdemaeker T, Wortmann R. *J. Am. Chem. Soc.* 2002; **124**: 9431–9447; (d) Kasha M, Rawls HR, El-Bayoumi MA. *Pure Appl. Chem.* 1965; **11**: 371–392; (e) Kasha M. In *Spectroscopy of the Excited State*, Bartolo B (ed.). Plenum: New York, 1976; 337–363.
44. Perrin DD, Armarego WLF. *Purification of Laboratory Chemicals* (3rd edn). Pergamon Press: Oxford, 1988.
45. Sheldrick GM. *Acta Crystallogr., Sect. A* 1990; **46**: 467.
46. Sheldrick GM. *SHELXL-97, Program for Crystal Structure Refinement*. University of Göttingen: Göttingen, 1997.
47. Flack HD. *Acta Crystallogr.* 1983; **A39**: 876.